THE PUBLISHING HOUSE
OF THE ROMANIAN ACADEMY

PROCEEDINGS OF THE ROMANIAN ACADEMY, Series A,
Volume 21, Number 2/2020, pp. 137–146

RESEARCH ON METHODS OF CHOOSING PLANAR NEAR-FIELD ACOUSTIC HOLOGRAPHIC REGULARIZATION PARAMETERS

Bingbing QI[1], Zhi LI[2], Xiaoguang LI[2], Huansheng ZHANG[3]

[1] Nanjing University of Aeronautics and Astronautics, College of Electronic and Information Engineering, 211106, China
[2] Harbin Engineering University, College of Underwater Acoustic Engineering, 150001, China
[3] The 3rd Research Institute of China Electronics Technology Group Corporation, 100015, China
Corresponding author: Bingbing QI, E-mail: 13699160512@163.com

Abstract. The regularization method for adaptive determination of angular spectrum filter parameters provides a powerful tool for engineering realization of near-field acoustic holography based on spatial acoustic field transformation. The basic Tikhonov regularization parameter selection method will be under-regularized at a relatively long holographic distance, which leads to the increase of reconstruction error. By improving the original Morozov deviation principle, using simple iteration to remove some high-wavenumber components of evanescent wave, and using the first-order Tikhonov filter, the suitable regularization parameters can still be obtained at a relatively long holographic distance. The numerical simulation shows that compared with the traditional regularization parameter selection method, the proposed regularization parameters can still be obtained. The reconstruction error is reduced by about 5%~9%.

Key words*:* NAH, STSF, Tikhonov regularization, MDP.

1. INTRODUCTION

NAH based on SFSF belongs to the inverse problem of pathological acoustics. For planar NAH evanescent wave, it decays exponentially and is amplified exponentially by inverse Green's function in the process of inverse reconstruction [1]. Small measurement noise may lead to the failure of acoustic field reconstruction. The earliest method to suppress noise is to apply an exponential lowpass filter to the reconstructed angular spectrum in the wavenumber domain. However, because of the need to select filter parameters manually, it has great limitations in practical engineering applications. In order to use regularization method, it is necessary to transform the reconstruction process of planar NAH into the expression of discrete transfer matrix. In planar NAH, the operator form of transfer matrix has the same unitary (orthogonal) property as the left and right matrices of singular value decomposition (SVD), which avoids the huge amount of SVD and saves computing time [2].

Tikhonov regularization adds smoothness constraints and suppresses noise amplification to some extent. The selection of regularization parameters is the key to the application of regularization. There are three mature methods: deviation principle method (MDP), generalized cross validation (GCV) and L-curve method. In reference [3], a more robust MDP method is used. By defining 1/4 of the angular spectrum of the hologram as the equivalent noise area, the noise power is estimated, and good reconstruction results are obtained within a certain holographic distance [4]. However, under the condition of long holographic distance, the leakage and winding errors caused by sound field truncation and sampling in reconstruction process will be much larger than the noise in measurement, and the noise estimation method given by this method is no longer applicable [5,6]. To solve this problem, an iterative noise power estimation method is proposed based on the fact that the plane angular spectrum energy is mostly concentrated in the low wavenumber region [7]. The basic idea is to estimate the dynamic range of the holographic angular spectrum and the cut-off wave-number of the equivalent noise region iteratively until some convergence criterion is satisfied, and then a more stable method is used [8,9]. The robust MDP method automatically selects the filter parameters and regularizes them according to the original idea. The numerical simulation results show that the improved MDP method (IMDP) can converge after several iterations, and can effectively suppress the winding effect and winding error at the expense of some evanescent waves with high wavenumber components. It achieves an ideal balance between resolution loss and noise suppression, which is conducive to the engineering realization of STSF-NAH.

2. BASIC THEORY OF PLANAR NAH

The angular spectrum $P_H(k_x,k_y)$ of the holographic surface sound pressure $p_H(x,y)$ in the plane NAH can be related to the product of the angular spectrum $P_S(k_x,k_y)$ of the reconstructed surface sound pressure $p_S(x,y)$ and the Dirichlet Green's function (domain), namely:

$$P_H(k_x,k_y) = P_S(k_x,k_y)G_D(k_x,k_y), \tag{1}$$

$$P_{H,S}(k_x,k_y) = \iint_{-\infty}^{+\infty} p_{H,S}(x,y)e^{-i(k_x x+k_y y)}\mathrm{d}x\mathrm{d}y, \tag{2}$$

$$p_{H,S}(x,y) = \frac{1}{4\pi^2}\iint_{-\infty}^{+\infty} P_{H,S}(k_x,k_y)e^{i(k_x x+k_y y)}\mathrm{d}k_x\mathrm{d}k_y, \tag{3}$$

$$G_D(k_x,k_y) = e^{i\sqrt{k^2-k_\rho^2}\,d}, \quad k_\rho^2 = \sqrt{k_x^2+k_y^2}. \tag{4}$$

d is a positive number indicating the distance between two holographic surfaces.

In order to use the regularization method, the reconstruction process of the planar NAH needs to be converted into a transfer matrix representation, that is:

$$p_H = \mathbf{H}p_S. \tag{5}$$

$\mathbf{H}$ denotes the transfer matrix, containing the two-dimensional DFT operator and the Green function operator. Its expression is:

$$\mathbf{H} = \mathbf{F}^{-1}\mathbf{G}\mathbf{F}, \tag{6}$$

where $\mathbf{F}$ denotes a DFT operator consisting of a one-dimensional DFT matrix $\mathbf{W}$, and satisfies the orthogonal relationship:

$$\mathbf{F}^H\mathbf{F} = \mathbf{I}_M, \quad \mathbf{F}^{-1} = \mathbf{F}^H, \tag{7}$$

$$\mathbf{W}_{kq} = \sqrt{1/N}\, e^{-i2\pi/Nkq}, \quad k,q = 0,1,\ldots,N-1. \tag{8}$$

$\mathbf{G}$ represents the Green function operator composed of the Dirichlet Green's function:

$$\mathbf{G} = \mathrm{diag}(\lambda_{11},\lambda_{12},\cdots\lambda_{ij}\cdots\lambda_{MM}), \tag{9}$$

$$\lambda_{ij} = e^{i\sqrt{k^2-k_{\rho ij}^2}\,d} \left(k_{\rho ij}^2 = \sqrt{k_{xi}^2+k_{yj}^2}\right). \tag{10}$$

The SVD of the transfer matrix is:

$$\mathbf{H} = \mathbf{U}\boldsymbol{\Sigma}\mathbf{V}^H = \sum_{i=1}^{M}\sigma_i\mathbf{u}_i\mathbf{v}_i^H. \tag{11}$$

$\mathbf{U},\mathbf{V}$ represent left and right unit unitary (orthogonal) matrices. Then we obtain $\mathbf{U}^H\mathbf{U} = \mathbf{I}_M$, $\mathbf{V}^H\mathbf{V} = \mathbf{I}_M$; $\boldsymbol{\Sigma}$ represents a diagonal matrix composed of monotonically decreasing non-negative real singular values, then by comparing equations (6) and (11) we find:

$$\mathbf{U} \Leftrightarrow \mathbf{F}^H = \mathbf{F}^{-1},\ \ \mathbf{V}^H \Leftrightarrow \mathbf{F},\ \ \mathbf{\Sigma}^2 = \mathbf{G}^H\mathbf{G}\,. \tag{12}$$

Unlike the conventional SVD, the singular value λ_{ij} corresponding to the DFT decomposition is plural. The least squares solution of the reconstructed surface sound pressure is obtained by inverting equation (5) as:

$$p_s = (\mathbf{H}^H\mathbf{H})^{-1}\mathbf{H}^H p_H = \sum_{i=1}^{M} \frac{\mathbf{u}_i^H p_H}{\sigma_i}\mathbf{v}_i\,. \tag{13}$$

According to the equation (9) and (10), the singular value of the evanescent wave ($k^2 < k_{\rho ij}^2$) attenuated.

The matrix $\mathbf{H}$ condition number is:

$$\mathrm{cond}(\mathbf{H}) = |\sigma_1| / |\sigma_M| = e^{d\sqrt{(\pi/\Delta x)^2 + (\pi/\Delta y)^2 - k^2}}\,. \tag{14}$$

As the holographic distance increases, the condition number of $\mathbf{H}$ increases exponentially. The transfer matrix $\mathbf{H}$ is highly ill-conditioned, and solving the sound field at the reconstructed surface by the equation will inevitably produce a huge error.

3. REGULARIZATION

3.1. Tikhonov regularization

It is assumed that the error of p_H^δ in the holographic sound pressure is a spatially uncorrelated Gaussian noise ε ith zero mean, and the standard deviation is σ, which has the following relationship with the reconstructed sound pressure p_H^δ:

$$p_H^\delta = \mathbf{H}p_s^\delta,\ \ p_H^\delta = p_H + \varepsilon\,, \tag{15}$$

$$E\left\| p_H^\delta - p_H \right\| = \sigma\sqrt{M}\,. \tag{16}$$

The Tikhonov regularization imposes a certain smoothness constraint on the amount of solution, so that the weighted sum of the residual norm $\left\|\mathbf{H}p_s^\delta - p_H^\delta\right\|$ and the solution norm $\left\|\mathbf{L}p_s^\delta\right\|$ is minimum, namely:

$$J_\alpha(p_s^\delta) = \min\left\{ \left\|\mathbf{H}p_s^\delta - p_H^\delta\right\|^2 + \alpha\left\|\mathbf{L}p_H^\delta\right\|^2 \right\} \tag{17}$$

where, the second term is a penalty matrix, usually a (semi)positive definite matrix; $\mathbf{L}_M$ can be taken as the identity matrix $\mathbf{I}_M$, and $\alpha(\alpha \geq 0)$ denotes a regularization parameter. So, the standard regularization solution is:

$$p_s^{\alpha,\delta} = (\mathbf{H}^H\mathbf{H} + \alpha\mathbf{I})^{-1}\mathbf{H}^H p_H^\delta\,. \tag{18}$$

The SVD can be written as:

$$p_s^{\alpha,\delta} = \mathbf{F}^{-1}F^\alpha\mathbf{G}^{-1}\mathbf{F}p_H{}^\delta = \mathbf{V}F^\alpha \mathrm{diag}\left(\frac{1}{\lambda_1}, \frac{1}{\lambda_2}\cdots\frac{1}{\lambda_M}\right)\mathbf{U}^H p_H^\delta \tag{19}$$

where F^α denotes a low-pass filter with regularization parameters, then:

$$F^\alpha = \mathrm{diag}\left(\frac{|\lambda_1|^2}{\alpha + |\lambda_1|^2}, \cdots\frac{|\lambda_i|^2}{\alpha + |\lambda_i|^2}\cdots\frac{|\lambda_M|^2}{\alpha + |\lambda_M|^2}\right). \tag{20}$$

If α is too small, the error of high wavenumber components will be seriously amplified by the inverse Green function in the form of positive exponential, which makes the reconstruction results worse or even totally unreliable. If it is too large, it means that too much high wavenumber information of the reconstructed sound field is filtered out, and the reconstructed sound field is too smooth, which reduces the spatial resolution of the reconstructed results. In order to obtain high precision reconstructed sound pressure, the key is to select appropriate regularization parameters.

3.2. Morozov Deviation Principle (MDP)

The basic idea of the MDP is to satisfy the residual norm of the reconstructed sound field exactly equal to the noise power with a suitable regularization parameter:

$$\left\| \mathbf{U}(\mathbf{I} - F^{\alpha})\mathbf{U}^{H} p^{\delta} \right\| = \left\| F_1^{\alpha} \overline{p}^{\delta} \right\| = \sigma\sqrt{M} , \tag{21}$$

where:

$$\overline{p}^{\delta} \equiv \mathbf{U}^{H} p^{\delta} \tag{22}$$

$$F_1^{\alpha} = \mathbf{I} - F^{\alpha} = \mathrm{diag}\left(\frac{\alpha}{\alpha + |\lambda_1|^2}, \cdots \frac{\alpha}{\alpha + |\lambda_i|^2} \cdots \frac{\alpha}{\alpha + |\lambda_M|^2} \right) \tag{23}$$

indicates a high-pass filter corresponding to F^{α}. For the high wavenumber part, the value is close to 1, and the low wavenumber part approaches 0.

In the practical application of planar NAH, as shown in Fig. 1. the noise region of the holographic angular spectrum is used to estimate the noise variance quickly:

$$\left\| \mathbf{U}_q^{H} p^{\delta} \right\| \Big/ \sqrt{Q} = \sigma, \;\; q \in \Omega , \tag{24}$$

where Ω represents the noise area, namely $k_p = \sqrt{k_x^2 + k_y^2} \geq \max\left(\frac{\pi}{\Delta_x}, \frac{\pi}{\Delta_y} \right)$; Q represents the number of eigenvalues in the region.

The windowing effect and winding error caused by windowed truncation in spatial domain cannot be expressed by mean and variance. When the holographic distance is measured, it will be amplified sharply, which will cause the fluctuation of the reconstructed sound field. However, the traditional MDP only uses 1/4 of the equivalent noise variance of the holographic angular spectrum, which leads to under-filtering and cannot effectively suppress the error caused by windowing.

3.3. Iterative Discrepancy Principle

In many cases, for the holographic angular spectrum, it has a large low wavenumber component, and its component decreases rapidly as the wavenumber increases.

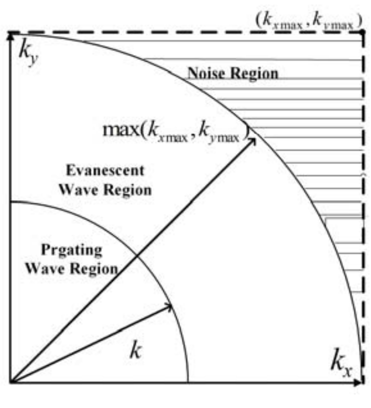

Fig. 1 – Schematic of holographic corner spectrum 1/4 equivalent noise.

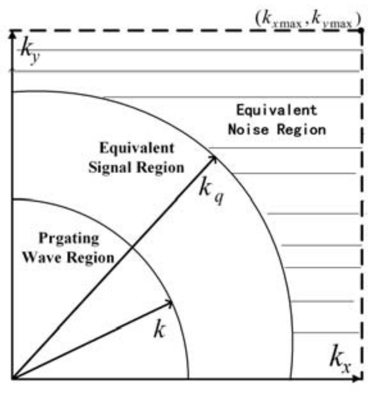

Fig. 2 – Schematic of holographic corner. spectrum equivalent noise.

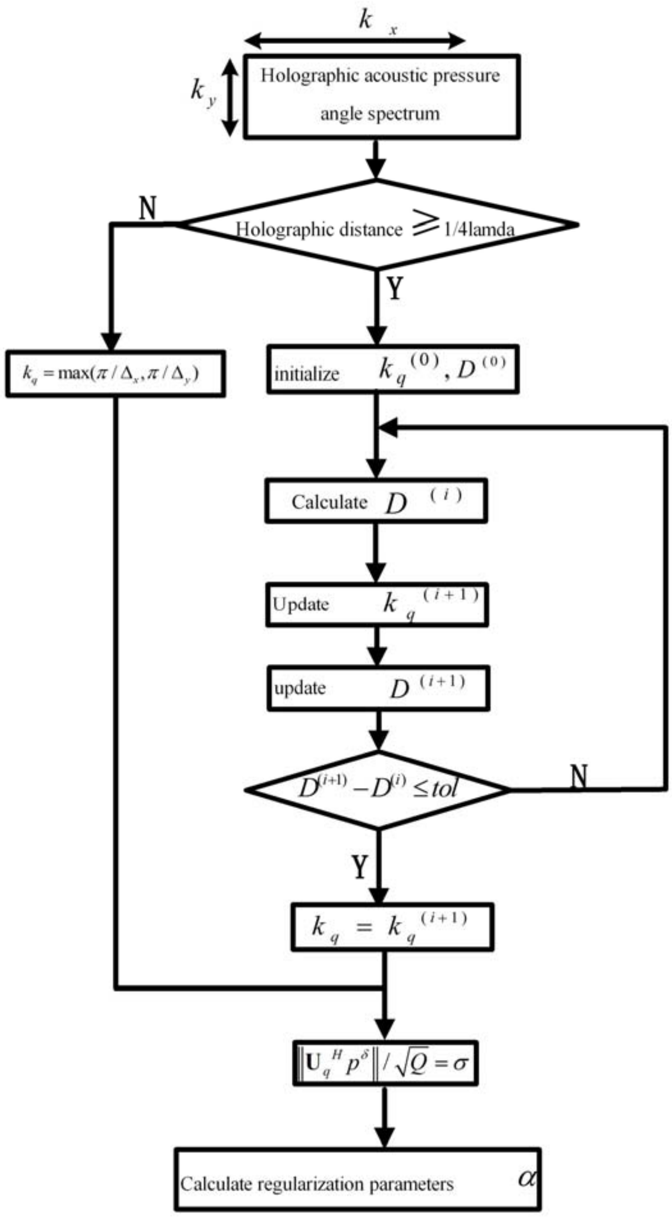

Fig. 3 – Diagram of the improved discrepancy principle method.

In order to consider the error caused by the window effect, the equivalent variance of the noise can be reestimated. The area of Fig. 1 is redivided to define $k_x^2 + k_y^2 \leq k_q^2$ as the equivalent signal area, and $k_x^2 + k_y^2 > k_q^2$ is the equivalent noise area, where k_q is the equivalent cut-off wave number. As shown in Fig. 2, k_q should satisfy the following equation according to reference [1]:

$$10^{D/20} \geq e^{\sqrt{k_q^2 - k^2}(z_H - z_s)}, \tag{25}$$

where D (in decibels) represents the dynamic range or the signal-to-noise ratio (SNR) of the test system. In practice D is generally difficult to obtain, and here we offer a method to iteratively solve the equivalent cut-off wave number k_q:

$$k_q^{(i+1)} = \sqrt{k^2 + \left[\frac{D^{(i)} \ln 10}{20(z_H - z_s)}\right]^2}, \tag{26}$$

$$D^{(i)} = 10\log_{10}\frac{\left\|\mathbf{U}^{H} p_{H}{}^{\delta}\right\|^{2} - \left\|\mathbf{U}_{q^{(i)}} p_{H}{}^{\delta}\right\|^{2}}{\left\|\mathbf{U}_{q^{(i)}} p_{H}{}^{\delta}\right\|^{2}}, \quad q^{(i)} \in \Omega^{(i)}, \tag{27}$$

where: $\Omega^{(i)}$ denotes the noise region represented $k_x^2 + k_y^2 \le k_q^{(i)2}$ and the initial value of $k_q^{(i)}$ is $k_q^{(0)} = \max(\pi/\Delta x, \pi/\Delta y)$. Its iterative process is shown in Fig. 3.

Experience shows that as the estimated value of the two adjacent iterations in the dynamic range of the holographic surface is less than or equal to 2 dB, terminating iteration is appropriate, and the reconstructed sound field with better accuracy can be obtained.

The IMDP method effectively suppresses the window effect and the amplification of the winding error at the expense of a small amount of spatial resolution, and obtains a relatively smooth reconstructed sound field. Also, it has achieved an ideal compromise between resolution loss and noise suppression, improving the accuracy of sound source recognition.

4. NUMERICAL SIMULATION

Near-field acoustic holography with equivalent source is used to calculate the equivalent source intensity by measuring the sound field information on the holographic plane. The sound field at the reconstruction plane is obtained by weighted superposition of the source intensity generated by a series of equivalent sources placed inside the vibration body. The winding error caused by wavenumber domain sampling is avoided fundamentally, and the reconstruction accuracy is high. In this section, “60% filtering parameters”, “traditional MDP (MDP)”, “improved MDP (IMDP)” and “equivalent source (ESM)” methods are used to compare and illustrate the advantages of the proposed method.

Relative root mean square error between reconstructed value and theoretical value is defined as reconstruction error:

$$\mathrm{Err} = \sqrt{\frac{\Sigma\left|p_s - \hat{p}_s\right|^2}{\Sigma\left|p_s\right|^2}} \times 100\% \tag{28}$$

In the formula, p_s is theoretical value of the sound pressure on the reconstructed surface, $\hat{p}_s$ is the reconstructed value of the sound pressure on the reconstructed surface.

Two in-phase pulsating spherical sound sources are selected, with the frequency of $f = 1\,000\ \mathrm{Hz}$, the pulsating sphere radius of $r_0 = 0.001\,\mathrm{m}$, the surface vibration velocity of $2.5\,\mathrm{m/s}$, and the pulsating sphere center positions of $(0.2\,\mathrm{m}, 0, 0)$ and $(-0.2\,\mathrm{m}, 0, 0)$; the holographic surface size is $1.0\,\mathrm{m} \times 1.0\,\mathrm{m}$, the number of holographic surface microphone measuring points is 21×21; the distance between the holographic surface and the sound source is $z_H = 12.5\,\mathrm{cm}$, and the distance between the reconstructed surface and the sound source is $z_S = 3.5\,\mathrm{cm}$; the Gaussian white noise with $\mathrm{SNR} = 30\,\mathrm{dB}$ is added to the simulation, and the sound pressure is reconstructed by planar NAH technology.

Figure 4 shows the sound field distribution reconstructed via classical filter parameters (60%). Different colours represent numerical values. Thus the cut-off wave number is chosen to be 60% of the highest wave number by empirical value, i.e. $k_c = 0.6\pi/\Delta$. As indicated, (a) is the sound pressure amplitude; (b) is the sound pressure phase. It is observed that the error caused by the winding effect is amplified during the reconstruction process. Consequently, less filter causes larger edge fluctuation of the reconstructed surface sound pressure.

Figure 5 shows the sound field distribution reconstructed via the traditional MDP criterion in reference [3]. As indicated, (a) is the sound pressure amplitude; (b) is the sound pressure phase. As the holographic distance is far ($z_h = 12.5\,\mathrm{cm} > 11.3\,\mathrm{cm} = \lambda/3$), the partial error power of the holographic surface spectrum causes underestimation of the error term at the right end of the MDP, leading to less filter parameters, resulting in a sharp amplification of the winding error during the reconstruction process.

a) sound pressure amplitude b) sound pressure phase

Fig. 4 – Reconstructed sound field of reconstructed surface (60%).

a) sound pressure amplitude b) sound pressure phase

Fig. 5 – Reconstructed sound field of reconstructed surface (MDP).

Figure 6 presents a sound field distribution reconstructed via the improved MDP criteria herein. As indicated: a) is the sound pressure amplitude; b) is the sound pressure phase.

The equivalent source method (ESM) is used to reconstruct the sound field distribution (Fig. 7). 21×21 equivalent sources are arranged on the plane 1 cm away from the sound source, and the regularization parameters are selected by GCV criterion. As indicated: a) is the sound pressure amplitude; b) is the sound pressure phase.

a) sound pressure amplitude b) sound pressure phase

Fig. 6 – Reconstructed sound field of reconstructed surface (IMDP).

a) sound pressure amplitude b) sound pressure phase

Fig. 7 – Reconstructed sound field of reconstructed surface (ESM).

Figure 8 shows the sound field distribution at $y=0$ (sound pressure amplitude). It is observed that the IMDP method and the ESM method are most similar, and this outcome is basically consistent with the reconstruction percentage error given in Table 1.

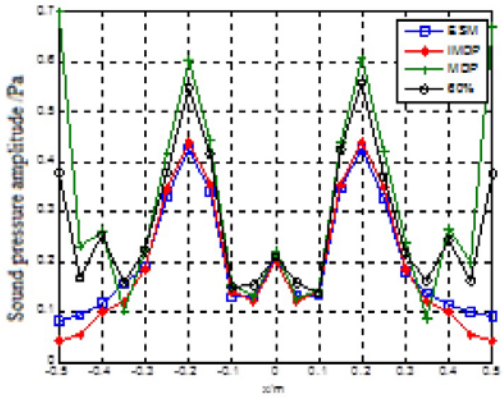

Fig. 8 – Contrast of sound fields of reconstructed surface.

Table 1

Reconstruction errors contrast of different reconstructing methods of pulsating ball sound source

Reconstruction error	60%	MDP	IMDP	ESM
Center	33.6.	53.3	26.8	7.3
Whole	58.3	107.7	36.5	10.2

5. EXPERIMENT

The experiment generates a single-frequency signal with a frequency of 500 Hz and an amplitude of 2-Vrms through the signal acquisition board, which stimulates the speaker to produce a steady-state sound field.

In the test, each speaker only sounds in the paper cone, as shown in Fig. 9.

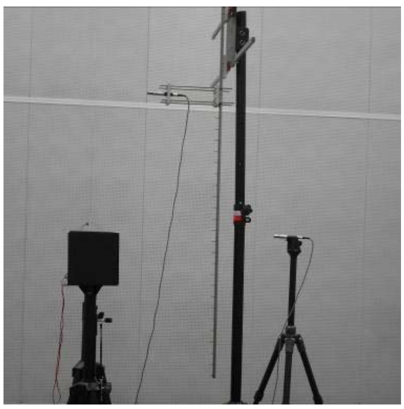

Fig. 9 – Experiment.

Figure 10 shows the spatial domain distribution of the measured sound pressure amplitude and phase, where: a) is the amplitude distribution and b) is the phase distribution. As indicated, the measured value only barely distinguishes the position of the main sound source under the influence of noise pollution and coherent source, but it needs to be further processed to obtain the position information of the main sound source.

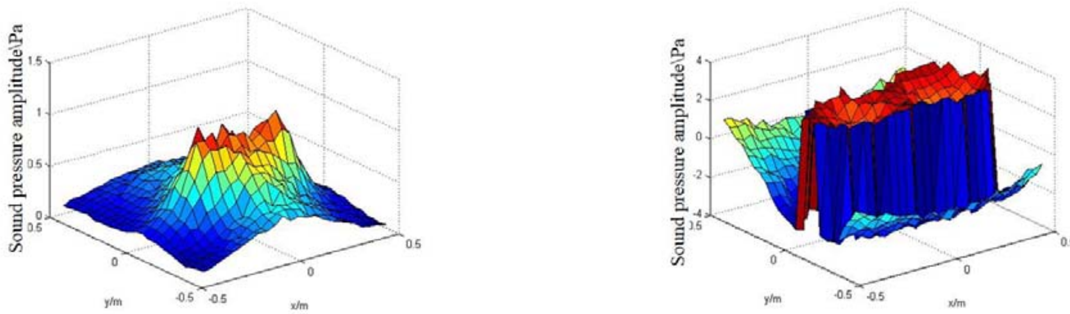

a) sound pressure amplitude measurement b) sound pressure phase measurement

Fig. 10 – Spatial distribution of holographic surface sound pressure.

Figure 11 indicates the distribution of sound pressure amplitude on the reconstructed surface obtained via four algorithms. The advantages of the proposed method are also illustrated using the 60% filtering parameters, MDP, IMDP and ESM methods.

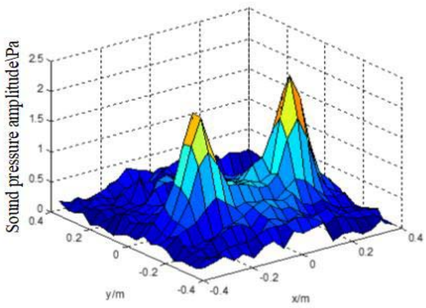

a) 60%

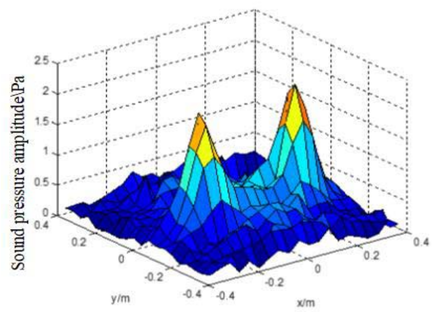

b) MDP

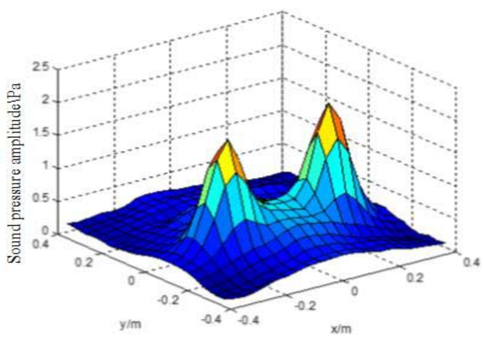

c) IMDP

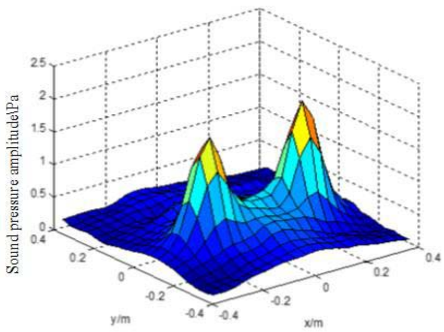

d)

Fig. 11 – Spatial distribution of holographic surface sound pressure.

6. CONCLUSIONS

The MDP criterion of adaptive deterministic domain filter is given in reference [3]. However, under-filtering will occur at a long holographic distance, which will lead to larger fluctuations in the reconstructed sound field and lower reconstruction accuracy. Based on the fact that the angular spectrum energy is mostly concentrated in low wavenumber components, an iterative estimation method of noise power is proposed in this paper. The numerical simulation results show that the improved deviation principle (IMDP) can reconstruct relatively smooth sound field steadily and quickly under the condition of measuring a long holographic distance, and can effectively improve the noise power. It improves the reconstruction accuracy of sound field and is beneficial to the engineering realization of STSF-NAH.

REFERENCES

1. E.G. WILLIAMS, *Continuation of acoustic near-fields*, J. Acoustic. Soc. Am, **113**, *3*, pp. 1273-1281, 2003.
2. J.D. MAYNARD, E.G WILLIAMS, Y. LEE, *Nearfield acoustic holography: I. Theory of generalized holography and the development NAH*, J. Acoustic. Soc. Am., **78**, *4*, pp. 1395-1413, 1985.
3. E.G. WILLIAMS, *Regularization methods for near-field acoustical holography*, J. Acoustic. Soc. Am., **110**, *4*, pp. 1976-1988, 2001.
4. R. JEANS, I.C. MATHEW, *The wave superposition method as a robust technique for computing acoustic fields*, J. Acoustic. Soc. Am., **92**, *2*, pp. 1156-1166, 1992.
5. J. HALD, *STSF – a unique technique for scan-based near-field acoustic holography with restriction on coherence*, B&K Technical Review, 1989.
6. Yunan HE, Zuoyong HE, *Full spatial transformation of sound field based on planar acoustic holography: I. Principle and algorithm*, Acta Acustica, **27**, pp. 507-512, 2002.
7. Daliang CHEN, Gequn SHU, Haiqiao WEI, *Comparison of regularization methods of nearfield acoustic holography*, Journal of Tianjin University, **41**, pp. 697-702, 2008.
8. P.C. HANSEN, *Regularization tools: A Matlab package for analysis and solution of discrete ill-posed problem*, Numerical algorithms, **6**, *1*, pp. 1-35. 1994.
9. Liang XU, Chuanxing BI, Jian CHEN, Xinzhao CHEN, *Nearfield acoustic holography based on K-space data extrapolation method*, J Chinese Journal of Mechanical Engineering, **43**, pp. 85-90, 2007.

Received June 16, 2019